

# Brain Cytochrome Oxidase: Purification, Antibody Production, and Immunohistochemical/Histochemical Correlations in the CNS

Robert F. Hevner and Margaret T. T. Wong-Riley

Department of Anatomy and Cellular Biology, Medical College of Wisconsin, Milwaukee, Wisconsin 53226

**Cytochrome oxidase (CO) is a mitochondrial energy-generating enzyme used in brain studies as a marker of neural functional activity. The activity of CO in different brain regions, revealed histochemically, is distributed nonhomogeneously but in distinct patterns. Localized differences in CO activity could arise from localized differences in enzyme amount or from localized regulation of enzyme turnover number (molecular activity). To distinguish between these alternatives, we used antibodies against purified calf brain CO to assess the immunohistochemical distribution of CO amount (protein immunoreactivity) in several brain regions.**

Calf brain mitochondria (synaptic and nonsynaptic populations) were isolated from gray matter homogenates by differential centrifugation. CO was purified from detergent extracts of the mitochondria by cytochrome *c*-Sepharose 4B affinity chromatography. Antisera against the purified CO were raised in rabbits. The antibodies reacted specifically with CO, predominantly subunit IV, in SDS immunoblots. The antibodies did not react in SDS immunoblots with any other proteins solubilized from mitochondria or caudate nucleus but did cross-react with brain CO from other mammalian species and with bovine heart CO.

The immunohistochemical distribution of CO amount matched the histochemical distribution of CO activity in all regions tested, including the monkey hippocampus and the mouse olfactory bulb, somatosensory (barrel) cortex, and cerebellum. Thus, the amount of CO in neural tissue is distributed in the same nonhomogeneous pattern as the histochemical activity of CO. The results suggest that mechanisms exist by which CO molecules are selectively distributed within neurons to meet local metabolic demands posed by neural functional activity.

Neural functional activity is an energy-requiring process. Thus, the local rate of energy metabolism and the local level of functional activity are tightly coupled in the nervous system (Krnjevic, 1975; Sokoloff, 1984). This principle has been thoroughly demonstrated using the 2-deoxyglucose (2-DG) technique, in which the relative uptake of radiolabeled 2-DG (a glucose an-

alog) among brain regions is determined autoradiographically and correlated with the conditions of functional activity imposed during 2-DG administration (Sokoloff, 1984). Using this technique, it has been shown, for example, that when one eye is visually stimulated in primates, the rate of energy metabolism is higher in cortical ocular dominance columns corresponding to the stimulated versus the nonstimulated eye (Kennedy et al., 1976).

Not only is the rate of energy metabolism coupled to functional activity, but so also is the capacity for generating metabolic energy. The relative capacity for energy metabolism among brain regions is demonstrated using cytochrome oxidase histochemistry. Cytochrome oxidase (CO; ferrocyclochrome *c*/oxygen oxidoreductase, EC 1.9.3.1; for review, see Kadenbach et al., 1987) is the terminal complex of the mitochondrial respiratory chain, which generates ATP by oxidative phosphorylation. In CO histochemistry, the relative distribution of CO activity is visualized in tissue sections. The relative CO activity is an indicator of local tissue metabolic capacity, which is coupled to neural functional activity (reviewed by Wong-Riley, 1989).

In normal neural tissue, the capacity for energy metabolism, as revealed by CO histochemistry, varies so that different local tissue regions have different metabolic capacities. This variation occurs at the regional, laminar, cellular, and subcellular levels. This suggests that neural functional activity also varies locally, since CO activity is coupled to functional activity.

The local variations in CO activity are not random but follow a clear and reproducible pattern in a given brain region. For example, in the primate visual cortex, CO activity is highest in lamina 4C and forms a periodic pattern of puffs (also called patches or blobs) in laminae 2 and 3 (Horton and Hubel, 1981; Carroll and Wong-Riley, 1984; Horton, 1984). Physiological (Livingstone and Hubel, 1984) and 2-DG (Hendrickson and Wilson, 1979; Tootell et al., 1988) studies suggest that these regions of high CO activity are also regions of high functional activity. In the visual cortex and in other brain regions as well, the normal distribution of CO activity seems to reflect the coupling between energy metabolic capacity and neural functional activity (Wong-Riley, 1989).

The biochemical mechanisms linking functional activity and energy metabolic capacity somehow cause CO activity levels to vary locally within neural tissue. Regions of high CO total activity in brain tissue could contain larger amounts of CO protein, or the amount of CO might be the same, with individual enzyme molecules having a higher turnover number (molecular activity). The total activity of CO equals the product of these two factors (amount and turnover number). Many metabolic enzymes are known to be regulated at the level of amount (Schimke and

Received Mar. 3, 1989; revised Apr. 21, 1989; accepted Apr. 26, 1989.

This work was supported by NIH grants NS18122 and EY05439 (M.W.R.) and by the Medical Scientist Training Program at the Medical College of Wisconsin (R.F.H.). We thank Dr. Ed Krug for practical advice on our biochemical experiments, Dr. V. M. Haughton and Dr. C. Nguyen-minh for generously providing monkey brain tissue, Dr. A. Haas for critically reading the manuscript, and X. Luo, W. Kaboord, and S. Liu for assistance in the laboratory.

Correspondence should be addressed to Dr. Margaret T. T. Wong-Riley, Department of Anatomy and Cellular Biology, Medical College of Wisconsin, 8701 Watertown Plank Rd., Milwaukee, WI 53226.

Copyright © 1989 Society for Neuroscience 0270-6474/89/113884-15\$02.00/0

Doyle, 1970), whereas others are known to be regulated at the level of turnover number by such mechanisms as covalent modification (Cohen, 1980a, b).

The goal of this study was to distinguish whether mainly the amount or mainly the turnover number of CO is locally regulated in neural tissue. To determine the relative distribution of CO amount, antibodies against purified CO were generated and used to label CO immunohistochemically in brain tissue sections. The CO immunohistochemical pattern in each region was then compared with the CO histochemical pattern. Several brain regions known to have unique and characteristic patterns of CO activity were examined; these were the monkey hippocampus, and the mouse olfactory bulb, somatosensory (barrel) cortex, and cerebellum.

In each region tested, the CO immunohistochemical pattern matched the CO histochemical pattern. We conclude that CO molecules are distributed nonhomogeneously in neural tissue in a pattern that could account for the distribution of CO activity without postulating a major role for regulation of CO turnover number. A preliminary report of this work has appeared in abstract form (Hevner and Wong-Riley, 1987).

## Materials and Methods

**General chemicals.** Triton X-100, Triton X-114 (both polymers of polyoxyethylene p-t-octyl phenol), and Tween 20 (polyoxyethylene sorbitan monolaurate) were purchased from Sigma. Concentrations of these detergents are expressed as percentage (vol/vol). Horse heart (type III) and yeast (type VIII-B) cytochrome *c* also were from Sigma.

**Isolation of mitochondria.** Synaptic and nonsynaptic mitochondria were prepared from calf brain by the differential centrifugation procedure of Rendon and Masmoudi (1985), modified to accommodate a larger mass of tissue. For each preparation, 1 calf (16–17-week-old Holstein bull) brain was obtained fresh, packed in ice, and homogenized (Potter-Elvehjem type homogenizer) within 45 min postmortem. In order to minimize myelin contamination of the homogenate, only the cerebral cortex (scraped from the brain surface) and caudate nuclei were used as starting material. Their combined mass was usually ~120–150 gm.

Modifications to the procedure of Rendon and Masmoudi (1985) were made as follows. (1) After the first centrifugation step, the nuclear pellet was washed once to increase the recovery of mitochondria, since about one third of the CO activity was found in the first nuclear pellet. (2) The washed P2 pellet was resuspended in 120 or 180 ml of isolation buffer rather than 30 ml. (3) The washed synaptosomal fraction was lysed in 200 ml of hypotonic buffer rather than 40 ml.

**Solubilization of CO from isolated mitochondria.** Cytochrome *c*-depleted mitochondria were prepared from isolated mitochondria (50–150 mg protein) by the method of Jacobs and Sanadi (1960). Partially purified, solubilized CO was prepared from the cytochrome *c*-depleted mitochondria by the method of Jacobs et al. (1966a, b). The following modifications were made: (1) a higher concentration of Triton X-114 (0.006 ml 20% Triton X-114/mg protein) was used in the initial detergent extraction (this improved the subsequent CO purity and stability to desalting), and (2) the K phosphate ( $P_i$ ) concentration was increased to 0.5 M in the solubilization with Triton X-100 (this improved solubility and stability).

**Solubilization of commercially obtained bovine heart CO.** Bovine heart CO (Sigma) was solubilized in 0.5 M  $KP_i$ , pH 7.2 (KOH), 5% Triton X-100 on ice for 2–8 hr, at a concentration of 4 mg protein/ml. Lower salt or detergent concentrations failed to solubilize the enzyme, and higher detergent concentrations led to loss of enzyme activity. Insoluble material was removed by centrifugation at 105,000 *g* (max) for 60 min at 4°C. More than 95% of the CO activity remained in the supernatant. The specific heme a content of the enzyme obtained from Sigma was 1.0 nmol heme a/mg protein.

**Purification of CO.** All procedures were at 0–4°C. Solubilized crude heart or brain CO (5–15 mg protein) was desalted on a Sephadex G-100 (Pharmacia) column pre-equilibrated with 40 mM HEPES, pH 7.4 (KOH, pH 7.6 at 4°C), 0.05% Triton X-100. Fractions with CO activity were pooled and applied to a 1.5 × 3.7 cm column of yeast cytochrome

*c*-Sephacryl 4B (prepared by the method of Broger et al., 1986). The affinity column was pre-equilibrated with 40 mM HEPES, pH 7.4, 0.05% Triton X-100. The sample (5–10 mg protein) was applied to the column and washed with pre-equilibration buffer until the A280 nm and A405 nm (monitored with an ISCO Type 6 Optical Unit, UA-5 Absorbance Detector, and Model 1133 Multiplexer/Expander) returned to baseline. The column was further washed with 5–10 column volumes of 40 mM HEPES, pH 7.4, 0.5% Triton X-100, then eluted with 25 ml (total) of this buffer containing a linear gradient of 0–100 mM  $KP_i$ , pH 7.4 (KOH). The column flow rate was 2.1 cm/hr during the loading and elution steps and 4.3 cm/hr during the wash. Fractions (2 ml) were assayed for CO activity, cytochromes, conductivity (to estimate  $KP_i$ ), and protein.

**Biochemical assays.** Protein concentrations were determined spectrophotometrically in triplicate by the modified Bradford (1976) method of Read and Northcote (1981; dye-reagent no. 2) or by the BCA method (Pierce). The standard was BSA (Sigma).

CO activity was determined spectrophotometrically in triplicate at 30°C by the procedure of Wharton and Tzagoloff (1967), using the buffer system of Errede et al. (1978). The relation between cytochrome *c* oxidized versus cytochrome *aa*, added to the reaction was linear under these conditions. Activity was expressed as units, where 1 unit = 1  $\mu$ mol cytochrome *c* oxidized/min. The assay conditions are approximately saturating for CO, so no further kinetic analyses were performed in estimating turnover numbers (molecular activity).

Cytochromes were assayed spectrophotometrically by the procedure of Vannest (1966). Mitochondrial suspensions were solubilized in an equal volume of ice-cold 0.5 M  $KP_i$ , pH 7.4 (KOH), 5% Triton X-100. A minimum of 2 volumes of PBS (140 mM NaCl, 2.7 mM KCl, 1.5 mM  $KP_i$ , 8.1 mM  $Na_2P_i$ , pH 7.4) containing 4% Triton X-100 was then added to the mitochondria to ensure complete solubilization. The spectrophotometer chamber was cooled to 5°C to prevent aggregation, which occurred if the mitochondrial solution warmed.

**Electrophoresis.** Chemicals for electrophoresis were purchased from Bio-Rad or Research Organics. Urea-SDS-PAGE was by the procedure of Kadenbach et al. (1983), using a Bio-Rad Protean II apparatus and 1.5 mm thick gels. Gels were stained with 0.05% Serva blue R in 25% isopropanol, 10% acetic acid, or by the silver staining procedure of Wray et al. (1981) with glutaraldehyde (0.0125% in 50% methanol) enhancement (Dion and Pomenti, 1983). Molecular weight standards were purchased from Bio-Rad, BRL, or Amersham (prelabeled Rainbow standards). Subunits were identified using the nomenclature of Kadenbach et al. (1983).

Animal brain tissue samples were solubilized for electrophoretic and immunoblot analysis in 10% (wt/vol) SDS, at a ratio of 1 mg wet tissue/5  $\mu$ l 10% SDS, then further diluted into electrophoresis sample buffer. Brain tissue was assumed to contain 10% protein by weight (wet).

**Immunoblotting.** Proteins were transferred electrophoretically from polyacrylamide gels to nitrocellulose (Schleicher and Schuell type BA-83) by the procedure of Towbin et al. (1979) as modified by Kuhn-Nentwig and Kadenbach (1985), using a Bio-Rad Trans-Blot Cell. Kuhn-Nentwig and Kadenbach (1985) found that all CO subunits were transferred under their conditions. We did not assess transfer of CO subunits in our experiments but did observe that all molecular weight markers (as low as 6.2 kDa) were transferred. For immunolabeling, blots were blocked overnight at 4°C with 5% (wt/vol) nonfat dry milk in PBS (PBS-NFDM; Johnson et al., 1984). PBS-NFDM was also used for washes between antibody incubations and for antibody dilution. The blocked blot was incubated overnight at 4°C with primary antibody (anti-CO or preimmune serum at 1:2000), washed, then incubated with secondary antibody (Bio-Rad blotting grade goat anti-rabbit IgG, HRP conjugate, GaR-HRP, 1:2000) for 2–4 hr at room temperature. The blot was finally washed in PBS containing 0.2% Tween 20 (PBS-Tween) and developed for 5–15 min at room temperature with 0.01 mg/ml 4-chloro- $\alpha$ -naphthol, 0.01% (wt/vol)  $H_2O_2$ , in 1:5 methanol:PBS.

**ELISA assays.** All antibody titers were determined by ELISA. The titer was defined as the maximal dilution (lowest concentration) of anti-serum in which antibodies were detected. All ELISA incubations were at 4°C on a rotator. PBS-NFDM was used for washes between incubations (except where noted) and for dilutions of antibodies. Washes between incubations were done 3 times for 5 min. Controls (no primary antibody, preimmune serum) were run with every assay plate.

Polystyrene flat-bottom wells (Dynatech Immulon II) were coated overnight with 100  $\mu$ l/well purified CO (8.4 nmol heme a/mg protein) at 1  $\mu$ g/ml in 0.1 M  $NaHCO_3$ , pH 9.0. After coating with CO, the wells were blocked for 8 hr with 200  $\mu$ l PBS-NFDM. The wells were washed

and incubated with primary antibody (100  $\mu$ l/well, serial dilutions) for 8–12 hr. The wells were washed again and incubated with 100  $\mu$ l/well secondary antibody (Bio-Rad blotting grade GaR-HRP, 1:1000) for 8–12 hr. After a final wash with PBS-Tween, the assay was developed with 100  $\mu$ l/well 3.8 mM 2,2'-azino-bis(3-ethylbenzothiazoline-6-sulfonic acid), 0.03% (wt/vol) H<sub>2</sub>O<sub>2</sub>, in 0.1 M Na citrate, pH 4.2, for 30 min in the dark. The reaction was stopped by the addition of 25  $\mu$ l/well 10% (wt/vol) SDS. The A650 nm in each well was read on a Bio-Tek EL309 Microplate Autoreader.

**Antibody production.** Two female New Zealand White rabbits were immunized by the method of Hurn and Chantler (1980). One rabbit was selected for continued use of its antiserum based on its high antibody titer. This animal received a primary dose of 100  $\mu$ g purified (9.9 nmol heme a/mg protein) bovine brain CO emulsified with complete Freund's adjuvant (Difco) and injected at multiple intradermal and subcutaneous sites on the animal's back. The booster dose, containing 200  $\mu$ g purified brain CO (9.9 nmol heme a/mg protein) emulsified with complete Freund's adjuvant, was injected 10 weeks later at intramuscular sites in all four limbs. (The other animal was immunized by identical procedures but received primary and booster doses of 100  $\mu$ g and 50  $\mu$ g CO, respectively.) The rabbits were killed by sodium pentobarbital overdose.

IgG was purified from serum by DEAE-Affi Gel Blue chromatography (Bio-Rad) according to the manufacturer's instructions. IgG preparations were always used in CO immunohistochemistry, since background staining was lower. The anti-CO titer in IgG preparations was 20-fold less than that in sera because of dilution during chromatography. All anti-CO dilutions were normalized to the appropriate dilution of serum; e.g., IgG at 1:100 dilution was equivalent to serum at 1:2000 dilution. Serum and IgG preparations were stored frozen at  $-20^{\circ}\text{C}$  or  $-70^{\circ}\text{C}$  or lyophilized and frozen. Freezing and lyophilization did not affect anti-CO titers.

**Indirect immunoprecipitation.** Protein A-Sepharose CL-4B (Pharmacia;  $\sim 2$  mg protein A/ml swollen gel) was hydrated in PBS and washed with PBS containing 1% Triton X-100. Serum (5–60  $\mu$ l of preimmune or anti-CO) was mixed in polypropylene microcentrifuge tubes with washed protein A-Sepharose CL-4B (20–70  $\mu$ l) and brought to a total volume of 192  $\mu$ l with PBS. The molar ratio of protein A IgG-binding sites/IgG in each tube was adjusted to  $>2$ , based on a protein A molecular mass of 42 kDa, and two IgG-binding sites per protein A (Surolija et al., 1982); and an IgG molecular mass of  $\sim 150$  kDa and concentration in serum of  $\sim 10$  mg/ml (Johnstone and Thorpe, 1982). Tubes containing protein A-Sepharose and serum were incubated on a rotator for 45 min at room temperature, then cooled on ice. To each tube, 8  $\mu$ l of solubilized crude heart or brain CO was added. The tubes were incubated for 60 min at  $4^{\circ}\text{C}$  on a rotator, centrifuged for  $\sim 5$  sec to pellet the Sepharose beads, and assayed for CO activity in the supernatant.

**Preabsorption of anti-CO.** Antibodies reactive with purified CO were solid-phase absorbed by affinity chromatography against CO-Sepharose 4B, followed by incubation with CO absorbed to ELISA plates.

In the affinity chromatography step, purified (9.7 nmol heme a/mg protein) calf brain CO (466  $\mu$ g) was coupled to 133  $\mu$ l swollen CNBr-activated Sepharose 4B (Pharmacia) according to the manufacturer's instructions, except that 0.1% Triton X-100 was added to all solutions. The coupling reaction was successful, since the green CO color remained with the beads. The CO-Sepharose beads were poured into a pipette tip to make a column of volume 90  $\mu$ l. The column was equilibrated at  $4^{\circ}\text{C}$  with PBS, 0.1% Triton X-100. Lyophilized anti-CO was dissolved in PBS, 0.1% Triton X-100, at a relative dilution of 1:20 and passed over the column at 200  $\mu$ l/hr. Fractions (67  $\mu$ l) were collected and tested for anti-CO by ELISA. Residual anti-CO was detected, so a second absorption step was used.

In the second step, polystyrene wells were coated with purified CO and blocked with PBS-NFDM as described for ELISA assays. Partially absorbed anti-CO from the first step was diluted with PBS-NFDM to a final relative concentration of 1:400 and incubated with the CO-coated wells (100  $\mu$ l/well) for 8 hr at  $4^{\circ}\text{C}$ . The absorbed anti-CO was recovered with a micropipette and used in immunohistochemical control experiments.

**Animal tissue preparation.** Six adult mice (4 BALB/c and 2 C57Bl) and 2 adult female bonnet macaque monkeys (2–3 kg *Macaca radiata*) were used for histologic studies. The monkeys received intraocular injections of TTX into the left eye as part of another study. The mice were killed by cervical dislocation. The monkeys were deeply anesthe-

tized (sodium pentobarbital, 65 mg/kg) and decapitated. Tissues were removed from the animals and fixed by immersion in 4% paraformaldehyde, 4% sucrose, 0.1 M NaP<sub>i</sub>, pH 7.4, on ice, with agitation. The tissue was kept at  $4^{\circ}\text{C}$  in all further work until sectioning. After fixation for 4–6 hr, the tissues were rinsed in 4% sucrose, 0.1 M NaP<sub>i</sub> buffer, pH 7.4, then equilibrated with buffer containing increasing sucrose concentrations (10%, 20%, 30%) as a cryoprotectant to prevent freezing artifact. Sections were cut at 15–30  $\mu$ m on a freezing microtome and placed in PBS on ice until further processed. Alternate sections of all tissues were designated for CO histochemistry and immunohistochemistry. Occasional sections were used for Nissl (1% cresyl violet) staining.

**CO histochemistry.** Sections were processed for CO histochemistry by the method of Wong-Riley (1979).

**CO immunohistochemistry.** Free-floating sections were blocked for 8–24 hr at  $4^{\circ}\text{C}$  in PBS-NFDM containing 1% Triton X-100 and 1–5% (vol/vol) normal goat serum (NGS). The sections were rinsed in PBS, then incubated in primary antibody (anti-CO at 1:2000–8000) or preimmune serum (at 1:2000–5000) diluted in PBS-NFDM with 1% Triton X-100 and 5% NGS, for 4 hr at room temperature, then for 8–24 hr at  $4^{\circ}\text{C}$ . The sections were rinsed, then incubated with secondary antibody (Bio-Rad blotting grade GaR-HRP or Boehringer Mannheim goat anti-rabbit IgG, fluorescein conjugate) at 1:100 in PBS-NFDM with 5% NGS for 6 hr at room temperature or overnight at  $4^{\circ}\text{C}$ . The sections were again rinsed. Sections for immunofluorescence were incubated in tertiary antibody (Boehringer Mannheim swine anti-goat IgG, fluorescein conjugate, 1:100 in PBS-NFDM with 5% NGS) for 8–12 hr at  $4^{\circ}\text{C}$ , rinsed, mounted in 9:1 glycerol:PBS (the PBS was adjusted to pH 9.0 with Na<sub>2</sub>CO<sub>3</sub> and contained 10 mg/ml of 1,4-phenylenediamine to decrease fluorescence quenching), and stored at  $4^{\circ}\text{C}$  in the dark until viewed. Sections for immunoperoxidase were rinsed in 0.1 M NaP<sub>i</sub>, pH 7.0 (NH<sub>4</sub>OH), then incubated in the same buffer with 0.5% (wt/vol) 3,3'-diaminobenzidine-4 HCl (DAB) and 0.004% (wt/vol) H<sub>2</sub>O<sub>2</sub> for 3–10 min at room temperature. The DAB-reacted sections were rinsed with PBS, then mounted and coverslipped by standard procedures.

Solutions for immunohistochemical studies were preserved with 0.01–0.1% (wt/vol) thimerosal (Sigma). All rinses between antibody incubations were 3–5 times for 5 min with PBS. Immunohistochemical controls (preimmune serum and no primary antibody) were run with all tissues and processed identically with other sections. The concentration of preimmune serum always equaled or exceeded that of anti-CO. All incubations included gentle agitation.

## Results

### Purification of CO from calf brain

A typical mitochondrial preparation from 131 gm (wet weight) of calf brain cortex and caudate nuclei yielded 115 mg of non-synaptic mitochondrial protein and 65 mg of synaptic mitochondrial protein. Separation of synaptic and nonsynaptic mitochondria was based on the density difference between synaptosomes and free (nonsynaptic) mitochondria. Synaptic mitochondria were then released from synaptosomes by hypotonic lysis (Rendon and Masmoudi, 1985). Electron microscopic examination revealed only mitochondria and no other recognizable subcellular organelles (e.g., myelin, synaptosomes) in our preparations (Fig. 1).

Both the synaptic and nonsynaptic mitochondrial populations were rich in CO activity and respiratory chain cytochromes (Table 1). CO comprised 8–9% of the mitochondrial protein, based on 10.0 nmol heme a/mg protein in purified CO (Meincke and Buse, 1985). Lai and Clark (1979) have reported cytochrome contents in synaptic and nonsynaptic rat brain mitochondria very different from those reported here. Our results probably reflect the better estimate, since the ratio of cytochromes *b/c*, was found to be  $\sim 2$  in our samples but not in those of Lai and Clark (1979). This value matches the known composition of the *bc*<sub>1</sub> complex (respiratory complex III) in mitochondria (Vanneste, 1966) and in isolation (Hatefi, 1978).

The polypeptide compositions of the 2 mitochondrial preparations, analyzed electrophoretically, differed very little (data

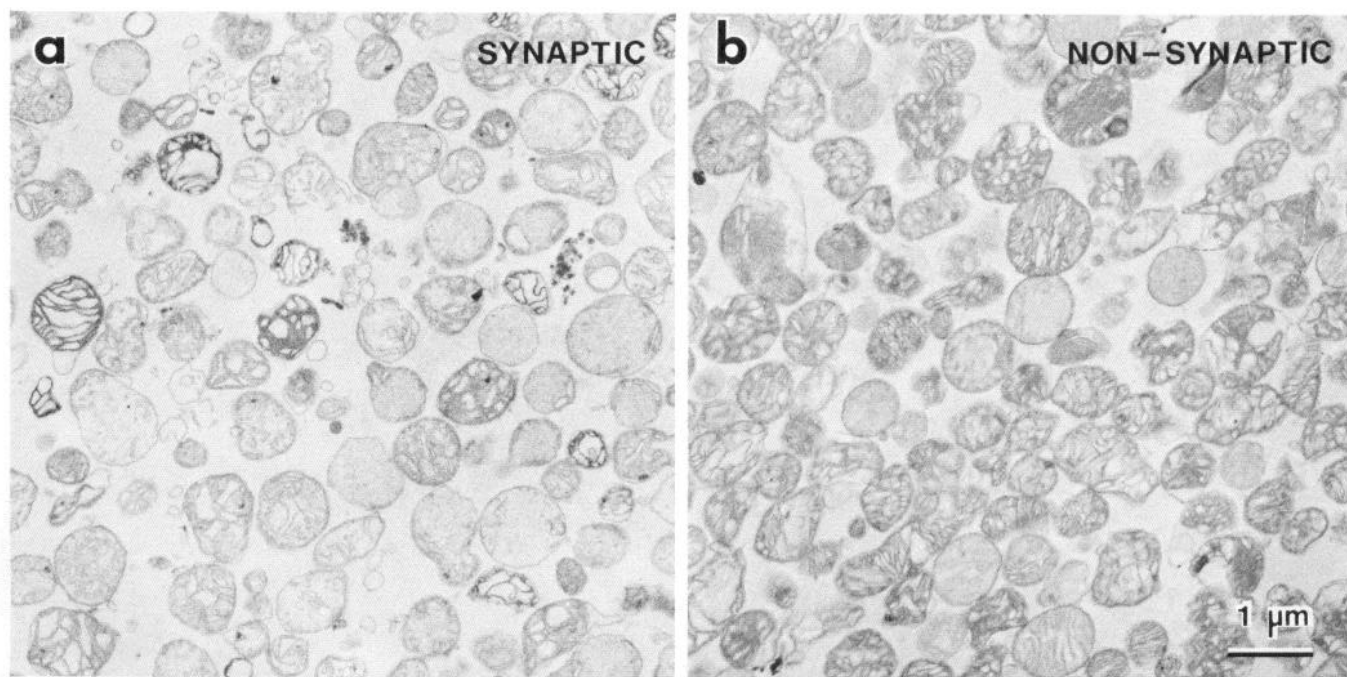


**Figure 1.** Mitochondria isolated from calf brain. The mitochondria were fixed in cold 2.5% paraformaldehyde, 1.5% glutaraldehyde, 4% sucrose, 0.1 M NaP<sub>i</sub>, pH 7.4, centrifuged to a pellet, osmicated, dehydrated, stained with uranyl acetate, embedded in Epon, and stained with lead citrate after thin sectioning. The synaptic mitochondria appear swollen compared with the nonsynaptic mitochondria, probably because of their exposure to hypotonic conditions during synaptosome lysis.

not shown). Only a few polypeptides (apparently unrelated to CO) seemed to be unique to one or the other mitochondrial population. In sum, both mitochondrial populations contained high levels of CO, differed little in their compositions, and appeared free of contamination by other organelles.

Results of a typical CO preparation from brain mitochondria are shown in Figure 2 and Table 2. Similar results were obtained in purifications of CO from bovine synaptic and nonsynaptic mitochondria and from crude bovine heart CO. The chromatographic profile (Fig. 2) shows that CO (measured as heme *a* in cytochromes *a* and *a*<sub>3</sub>, the spectrophotometrically detectable redox centers of CO) did not appear in any fractions during the loading or washing steps but only in elution fractions. The CO in this and other runs was eluted at KPi concentrations of 30–60 mM. Surprisingly, cytochrome *c* was also eluted by the salt gradient in every run, but cytochrome *bc*<sub>1</sub> never appeared in our

elution fractions. Cytochrome *bc*<sub>1</sub>, like CO, binds to cytochrome *c* and has been found in elution fractions by others using this method. Cytochrome *c* has not been reported previously in elution fractions (Kuhn-Nentwig and Kadenbach, 1985; Broger et al., 1986). Methodological differences probably account for these discrepancies.

Table 2 shows overall purification results from the same batch shown in Figure 2. From a relatively small quantity of brain mitochondria (46 mg protein), 400 μg CO were obtained at 99% purity (sufficient for immunizations). A striking loss of enzymatic activity occurred during the purification (Table 2), suggesting that the enzyme might have been denatured. However, Triton X-100 is known to inactivate CO by delipidation (Robinson and Capaldi, 1977) and, therefore, could also account for the loss of activity. Addition of soybean lecithin to the enzyme stimulated its activity severalfold (Table 2, Fig. 3), suggesting

**Table 1.** Cytochrome oxidase activity and cytochrome contents of mitochondria isolated from calf brain

Mitochondrial preparation <sup>a</sup>	Cytochrome oxidase specific activity (units/mg protein)		Specific content of mitochondrial cytochromes (nmol/mg protein)			
	Intact mitochondria	Disrupted <sup>b</sup> mitochondria				
			<i>aa</i> <sub>3</sub>	<i>b</i>	<i>c</i> <sub>1</sub>	<i>c</i>
Nonsynaptic A	0.77	5.39	0.907	0.353	0.170	0.532
Nonsynaptic B	0.84	7.50	0.846	0.366	0.180	0.513
Synaptic A	0.88	5.16	0.781	0.311	0.159	0.456
Synaptic B	1.34	5.86	0.800	0.324	0.162	0.341

<sup>a</sup> The letters A and B indicate separate preparations.

<sup>b</sup> Mitochondria were disrupted with an equal volume of 5% Triton X-100, 0.5 M KPi, pH 7.4.

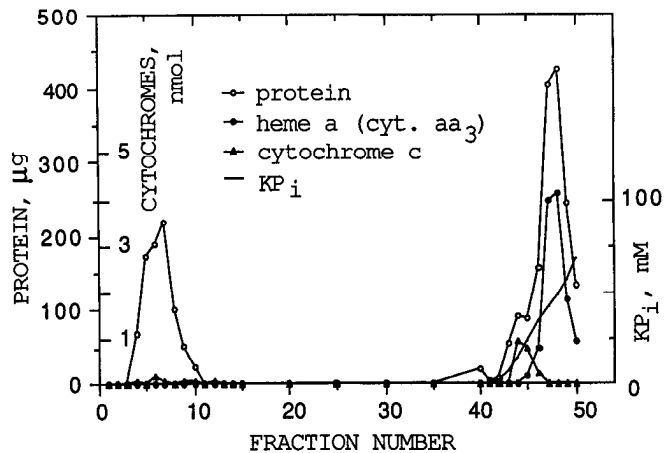


**Figure 2.** Cytochrome *c*-Sepharose 4B affinity chromatography purification of CO. Crude CO (5.6 mg protein) from brain nonsynaptic mitochondria was loaded on the column, washed with buffer, and eluted with a  $KP_i$  gradient (0–100 mM). Fractions (2 ml) were assayed for CO activity (not shown) in addition to the quantities shown. Some CO activity came through the column in the loading phase but in amounts too small to be detectable as heme *a*. The fractions rich in heme *a* also were rich in CO activity. Cytochromes *b* and *c*, were not detected in any fractions. The recovery of heme *a* in fractions 47–50 was 72% of that loaded.

that lipid depletion was indeed responsible for the decreased activity. Full activity might have been restored if we had used a more potent (and more expensive) phospholipid activator of CO (Vik and Capaldi, 1980).

Analysis by urea-SDS-PAGE did not reveal any subunit mobility differences between CO isolated from synaptic versus nonsynaptic mitochondria (Fig. 4), suggesting that both populations contained the same single isozyme. Differences were seen between brain and heart CO in the mobilities of subunits VIa (see Fig. 6*a*) and VIII (data not shown), indicating that isozyme differences were detectable in our system. CO from bovine tissues may contain up to 13 subunits (Kadenbach et al., 1983), but only 10 subunits were resolved on our gels. (Subunits VIIb and *c* appeared as a single band, as did subunits VIIa, *b*, and *c*.) A few faint bands in the higher molecular weight range of both gels could not be identified as CO subunits. Such bands may have represented aggregation products of hydrophobic subunits of the enzyme (Kadenbach et al., 1983) or impurities.

Given these uncertainties, heme *a*/protein ratios were the primary criterion used in assessing enzyme purity. The brain

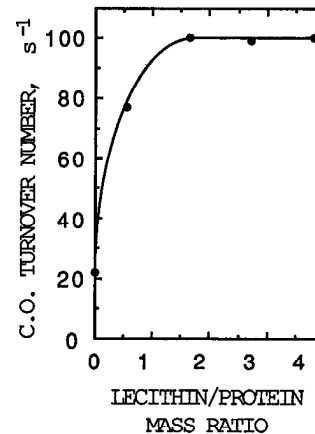


**Figure 3.** Activation of CO by soybean lecithin. Purified Triton X-100 solubilized brain CO (9.9 nmol heme *a*/mg protein) was sonicated for 5 sec with increasing amounts of crude lecithin (Sigma Type IV-S, soybean lecithin, 35% L- $\alpha$ -phosphatidylcholine) and assayed for activity. Control assays showed that the lecithin by itself contained no CO activity.

CO preparations were of high purity by the criterion of heme *a*/protein ratio and, as shown above, appeared to be homogeneous; i.e., only one isozyme of brain CO was detected.

#### Antibody specificity

All antibodies used in this study came from one rabbit. The anti-brain CO titer (all titers were determined by ELISA) in the animal's serum was undetectable before the first immunization, 1:50 in the week preceding the booster immunization, and 1:100,000 2 weeks after the booster (Fig. 5*a*). The titer remained at 1:100,000 in all subsequent bleeds, the last of which was taken 7 months after the booster. The antibodies had a similar titer against bovine heart CO (data not shown). Indirect immunoprecipitation experiments showed that the antibodies were capable of reacting with enzymatically active CO (Fig. 5*b*) as well as CO on ELISA plates. Active CO from both brain and heart was precipitated.

The antibodies not only reacted with CO, but also were specific for CO, as shown by SDS immunoblot analysis (Fig. 6*a*). The major immunoreactive band was identified as CO subunit IV based on (1) the presence of the band in lanes containing purified CO, and (2) the migration distance of the band, which was identical to that of CO subunit IV in silver-stained lanes from the same gel. Subunits I and II also showed slight immunoreactivity.

**Table 2.** Cytochrome oxidase purification from calf brain nonsynaptic mitochondria

Fraction	Protein (mg)	Heme a (nmol)	Purity <sup>a</sup> (nmol heme a/mg protein)	Yield (% heme a)	Turnover number (sec <sup>-1</sup> )
Mitochondria	45.9	38.9	0.9	100	33 (269) <sup>b</sup>
Applied to affinity column	5.6	15.1	2.7	39	168
Affinity chromatography fractions 47–50	1.2	10.9	9.1	28	21 (100) <sup>c</sup>
Affinity chromatography fraction 47	0.40	4.0	9.9	10	24 (100) <sup>c</sup>

<sup>a</sup> Purified CO contains 10 nmol heme *a*/mg protein.

<sup>b</sup> Activity after mitochondrial disruption with Triton X-100 given in parentheses.

<sup>c</sup> Activity after sonication with soybean lecithin given in parentheses.

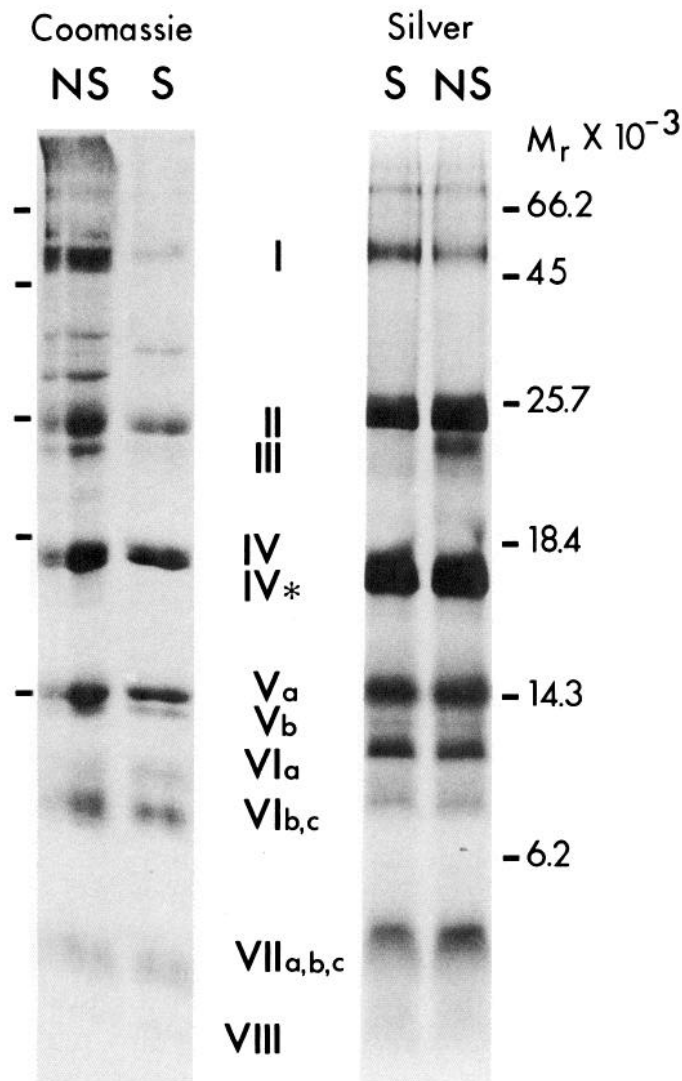


**Figure 4.** Subunit composition of CO purified from synaptic (S) and nonsynaptic (NS) mitochondria. The two gels (both 18.6% T, 3.0% C) contained different preparations of CO and were stained with Coomassie blue (Serva Blue R) or ammoniacal silver as indicated. Both gels are shown, since each highlighted different subunits more clearly. The positions of molecular weight markers are shown for each gel. Subunit III was not always visible in these or other gels. It is hydrophobic and sometimes aggregates during sample preparation. Subunits VIa and VIII are thought to be isozyme-specific but did not differ in their mobilities between the S and NS CO preparations. These subunits did show mobility differences between bovine brain and heart CO preparations (Fig. 6a and data not shown). In labeling the bands, it was assumed that 13 subunits were present but were not resolved (Kadenbach et al., 1983). The band labeled IV\* has been shown to be a proteolytic degradation product of subunit IV (Merle et al., 1981). Each lane contained 35  $\mu$ g protein on the Coomassie-stained gel and 7.5  $\mu$ g protein on the silver-stained gel.

As in the ELISA and indirect immunoprecipitation experiments, the antibodies reacted in immunoblots with both heart and brain CO (Fig. 6a). All of our immunohistochemical data thus agree in showing tissue cross-reactivity. A separate immunoblot experiment (Fig. 6b) showed that the antibodies also cross reacted with CO from different species. Brain CO subunit IV from monkey, mouse, cat, dog, rat, and even rabbit (in which species the antibodies were raised) were all immunoreactive. The detection limit of the immunoblot procedure (Fig. 6b) was between

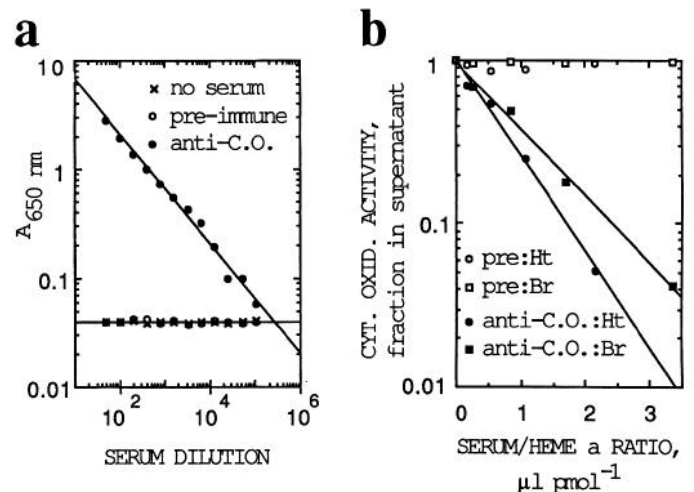


**Figure 5.** Detection of antibodies against CO. *a*, ELISA showing that antibodies to CO were detectable in antiserum diluted 1:100,000. Purified bovine brain CO was bound to polystyrene wells and allowed to react sequentially with anti-CO and GaR-HRP. The optical absorbance of the colored HRP reaction product was determined with a microplate reader. The antibodies also reacted with purified bovine heart CO in ELISA (not shown). *b*, Indirect immunoprecipitation of CO activity by anti-CO. The antibodies were bound to protein A-Sepharose CL-4B beads, then mixed with solubilized active CO from bovine heart (Ht) or brain (Br). The beads were pelleted, and CO activity was determined in the supernatant.

0.1–1.0  $\mu$ g calf brain CO holoenzyme, which corresponds to 8.4–84 ng subunit IV (Kadenbach et al., 1987).

To summarize, the anti-CO exhibited the following properties in biochemical tests: (1) high titer, (2) reactivity with both active and inactive CO, (3) specificity for CO, especially subunit IV; and (4) cross-reactivity among all mammals tested.

The antibodies also reacted specifically with CO in immunohistochemistry. Strong staining was seen in mouse and monkey brain tissues when anti-CO was used for immunohistochemistry but not when either anti-CO preabsorbed with CO or preimmune serum was used. Only low-level, nonspecific background staining was then seen (Fig. 7). Controls had low backgrounds whether the immunoperoxidase or the immunofluorescence method was used. The specificity and intensity of the immunohistochemical staining depended partly on the fixation and incubation conditions. Tissue fixed by perfusion or with glutaraldehyde usually had more nonspecific staining and less specific staining. Immersion fixation with paraformaldehyde always gave good results.

#### CO immunohistochemistry: correlation with histochemistry

Brain regions with well-defined, characteristic patterns of CO histochemical activity were selected for immunohistochemical analysis. The pattern of immunohistochemical labeling in each region was then compared with the pattern of CO histochemistry. In comparing the results, we refer to histochemical reactivity as “activity” of CO and to immunohistochemical reactivity as “amount” of CO. Reasons for equating immunohistochemical reactivity with CO amount will be given in the Discussion.

A typical and unmistakable match between the histochemical and immunohistochemical patterns was seen in the mouse somatosensory “barrel” cortex (Fig. 8). Both the activity and the amount of CO were enriched in the barrel hollows versus the

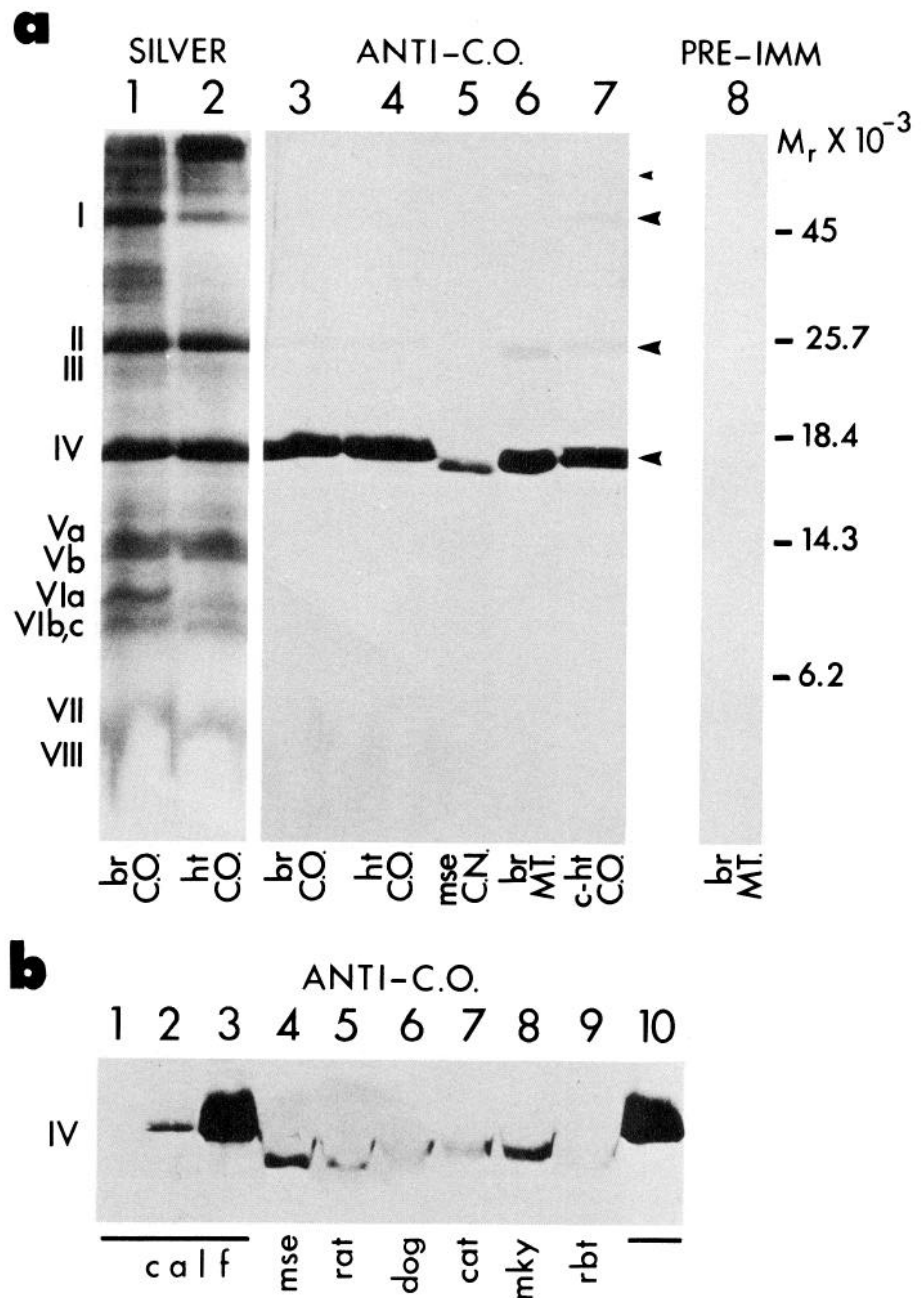


**Figure 6.** Immunoblot analysis of anti-CO specificity. *a*, Different lanes from the same gel (18.6% T, 3.0% C) were stained with silver to show CO subunits or transferred to nitrocellulose to show immunoreactive polypeptides, as indicated. Molecular weight marker positions are shown at the right. Bands immunoreactive with anti-CO are identified with large arrowheads; an unidentified immunoreactive band in lane 6 is indicated with a small arrowhead. This unidentified band appeared only in this lane and was relatively faint. It may have comprised aggregates of hydrophobic CO subunits. Note that brain (lane 1) and heart (lane 2) CO show a difference in the migration of subunit VIa. Lanes 1 and 3, 15  $\mu$ g partially purified bovine brain CO. Lanes 2 and 4, 15  $\mu$ g partially purified bovine heart CO. Lane 5, SDS-solubilized mouse caudate nucleus ( $\sim 50 \mu$ g protein). Lanes 6 and 8, SDS-solubilized brain mitochondria (50  $\mu$ g protein). Lane 7, crude bovine heart CO (40  $\mu$ g protein). *b*, The anti-CO recognized CO subunit IV in SDS-solubilized caudate nucleus from mouse (lane 4), rat (lane 5), dog (lane 6), cat (lane 7), monkey (lane 8), and rabbit (lane 9). Only subunit IV was visible in this blot. The slightly different mobilities of the immunoreactive bands probably reflect interspecies differences in the size of CO subunit IV. Lanes 1–3 and 10 contained purified bovine brain CO (lane 1: 0.1  $\mu$ g; lane 2: 1.0  $\mu$ g; lanes 3 and 10: 10  $\mu$ g). Lanes 4–9 each contained  $\sim 75 \mu$ g protein.

barrel septa, forming the well-known pattern of 5 barrel rows in the posteromedial barrel subfield (Woolsey and van der Loos, 1970). The only difference between the 2 patterns was that the CO histochemistry showed a higher degree of contrast between the hollows and septa than did the CO immunohistochemistry. This contrast difference between the 2 methods was found consistently in other brain regions as well.

In the mouse olfactory bulb, the patterns of CO amount (in this case shown as immunofluorescence) and CO activity again matched (Fig. 9). The plexiform layers and the glomeruli were most reactive, whereas the axon-rich regions and the mitral cell body layer were less reactive. Both staining methods revealed that not all glomeruli were equally rich in CO. Apparently, individual glomeruli maintain different levels of neural functional activity.

The distributions of CO histochemical and immunohistochemical labeling in the mouse cerebellum likewise matched and contrasted with the distribution of cell bodies, shown by a Nissl stain (Fig. 10). The cerebellum as a whole (Fig. 10*a–c*) had the highest levels of CO amount and activity in the cortex and deep nuclei. White matter (as is invariably the case) stained very lightly by both methods. Within the cerebellar cortex (Fig. 10*d–f*), the CO histochemical and immunohistochemical methods both showed punctate staining in the molecular layer, pericellular labeling around the Purkinje cells, and intense patchy staining in the granule cell layer. Cells in the molecular layer were visible by CO immunohistochemistry but not histochemistry. Examination of the deep cerebellar nuclei at higher magnification (Fig. 10*g–i*) revealed that high levels of CO amount and activity were present in neurons as well as in the neuropil.

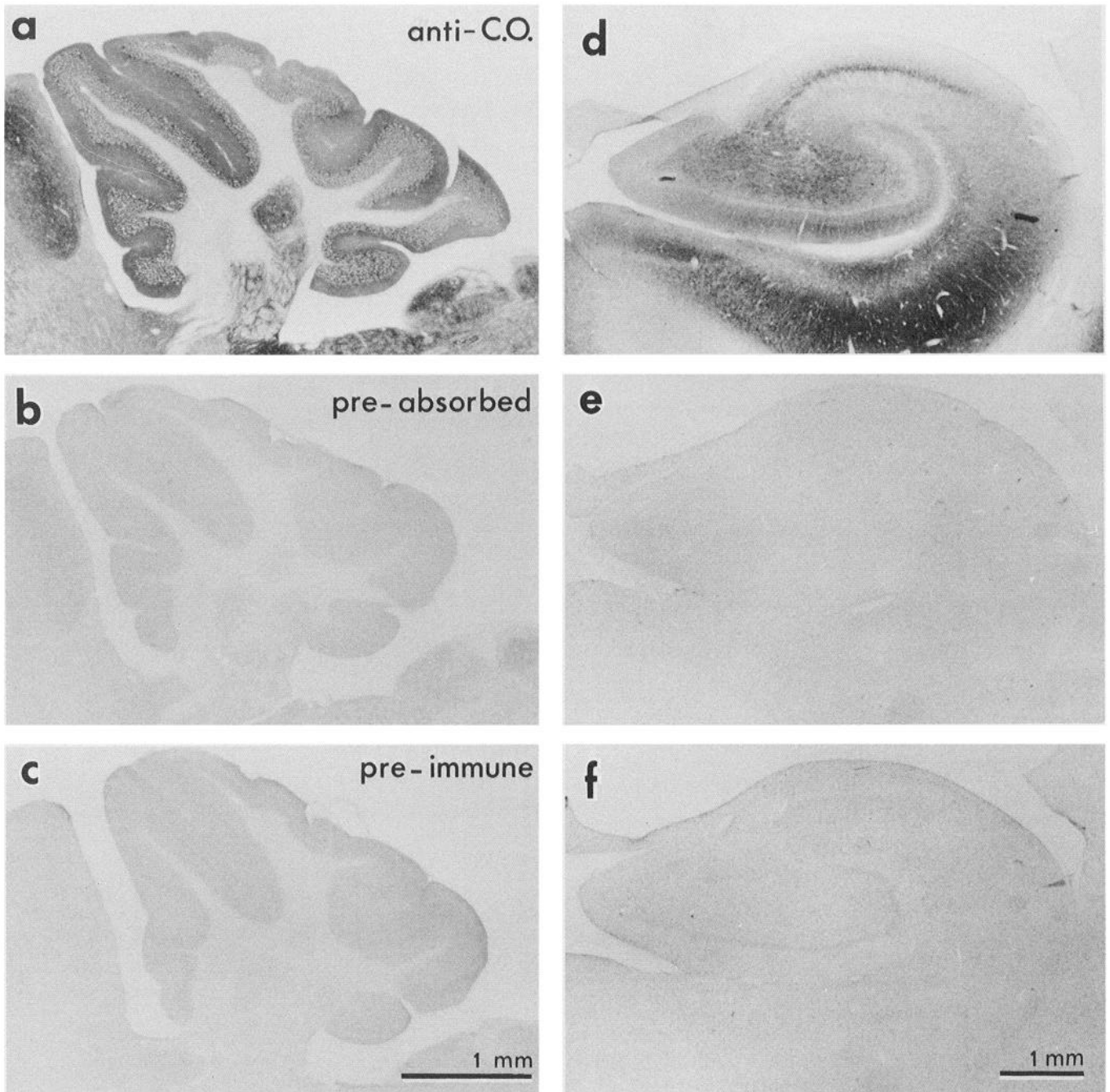


**Figure 7.** Specificity of CO immunohistochemistry in both the mouse and the monkey brain. Neighboring frozen sections from the same block of mouse cerebellum (*a-c*) or monkey hippocampus (*d-f*) were processed for immunohistochemistry with anti-CO (1:8000; *a* and *d*), anti-CO preabsorbed with purified CO (1:8000; *b* and *e*), or preimmune serum (1:5000; *c* and *f*). The sections were further incubated with GaR-HRP and reacted with DAB. Sections of cerebellum were cut in a parasagittal plane at 20  $\mu$ m. Hippocampus sections were cut perpendicular to the long axis of the formation at 30  $\mu$ m. The low-level nonspecific background staining seen in preimmune and preabsorbed control sections appeared at higher magnification to be localized to glial processes. Similar control results were obtained using the immunofluorescence method.

The pattern of CO histochemistry in the mouse cerebellum was very similar to that seen in a previous light and electron microscopic study of the rat cerebellum (Mjaatvedt and Wong-Riley, 1988). In that study, the punctate staining of the molecular layer was localized to Purkinje cell dendrites, the pericellular labeling around Purkinje cells was localized to presumptive basket cell terminals, and the patchy staining in the granule cell layer was localized to mossy fiber terminals. Presumably, these

same neuronal elements were CO-reactive histochemically and immunohistochemically in this study of the mouse.

The distributions of CO amount and activity in the monkey hippocampus were, as in regions of the mouse brain, very similar to each other, and very different from the distribution of cells (Fig. 11). The white matter regions all showed low CO levels, whereas the highest levels of CO amount and activity were seen in the outer portion of the dentate molecular layer, the CA3

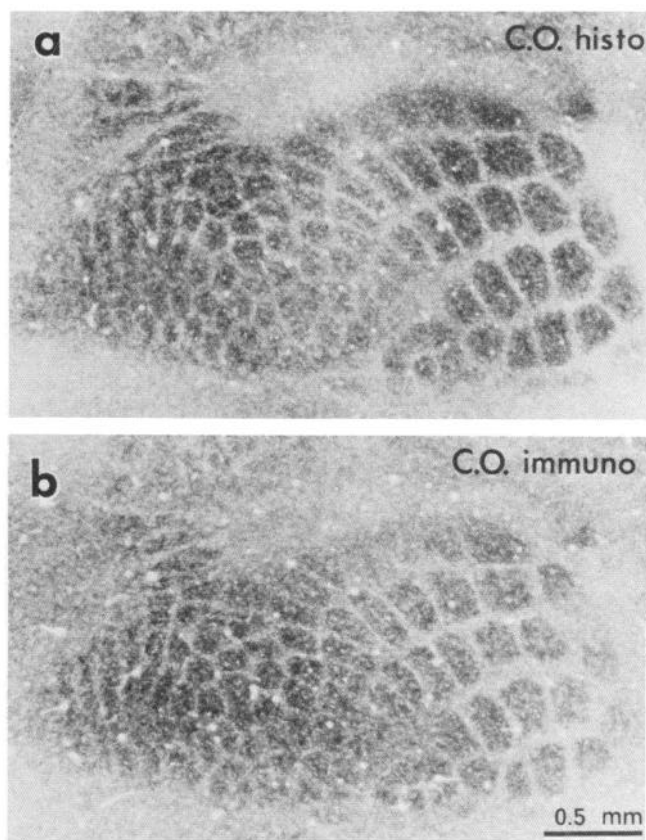


**Figure 8.** Correlation of CO activity and amount distributions in the mouse somatosensory (barrel) cortex. Adjacent frozen sections ( $20\ \mu\text{m}$ ) processed for CO histochemistry (*a*) and CO immunohistochemistry (*b*) are shown. Sections were cut in a plane tangential to the cortical surface; the cortex was flattened before sectioning. The section shown in *b* was incubated with anti-CO at 1:8000, then visualized with GaR-HRP and DAB. Both sections were photographed and printed with the same degree of contrast.

pyramidal cell layer, and the CA1 molecular layer. This same distribution of CO histochemical activity is found in the hippocampus of many mammalian species (Kageyama and Wong-Riley, 1982). Distinctive patterns of CO histochemistry are also found on a finer scale in several subregions of the hippocampus (Kageyama and Wong-Riley, 1982). These distinctive patterns were visible by both CO histochemistry and immunohistochemistry in this study.

In the dentate gyrus, for example, a marked difference was seen between the outer and inner portions of the molecular layer in both CO histochemical activity and CO immunohistochemical amount (Fig. 11). Darkly stained ascending dendrites were prominent in the outer but not the inner molecular layer of the dentate gyrus. As noted previously (Kageyama and Wong-Riley,

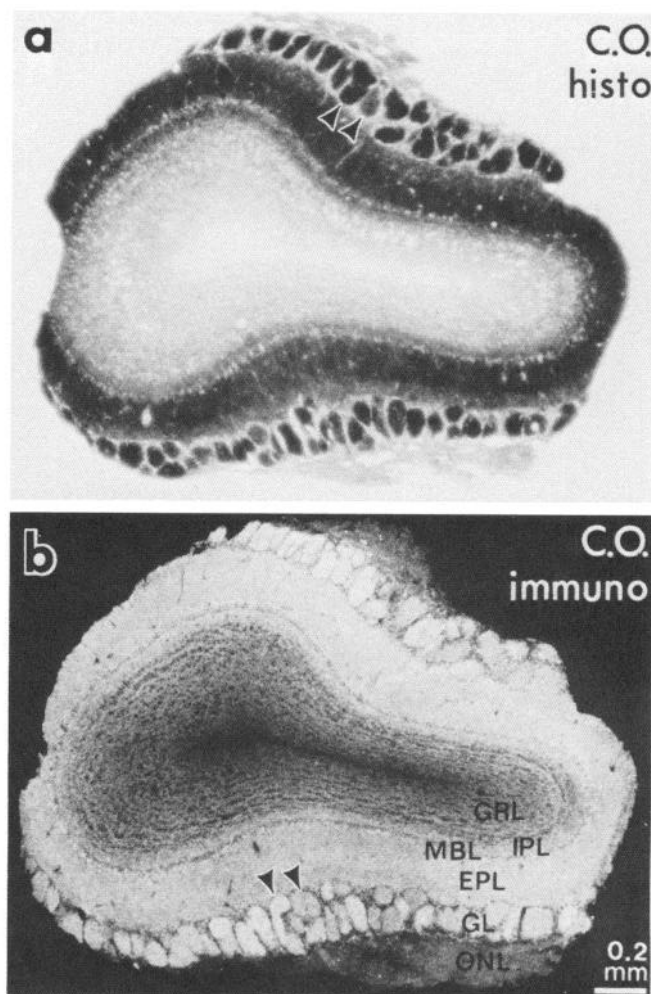
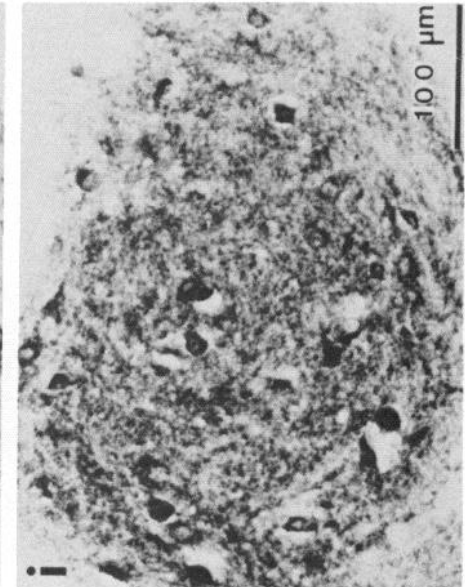
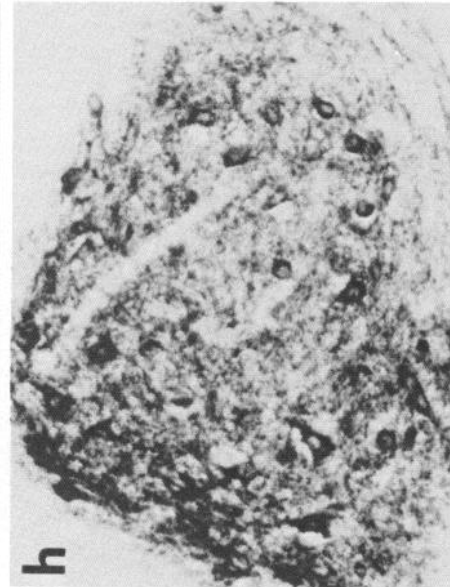
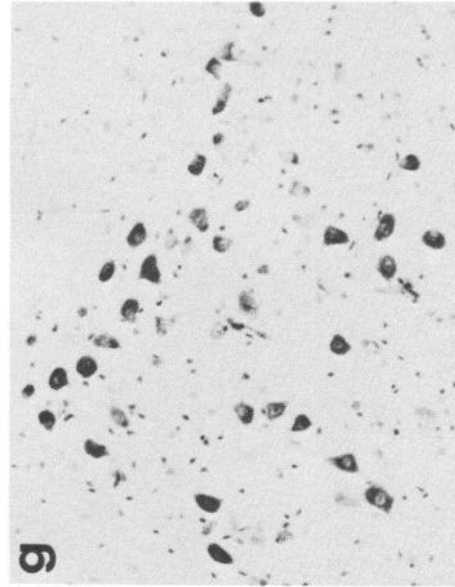
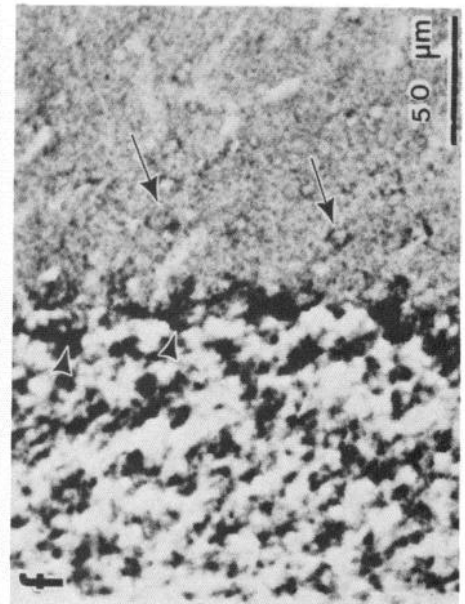
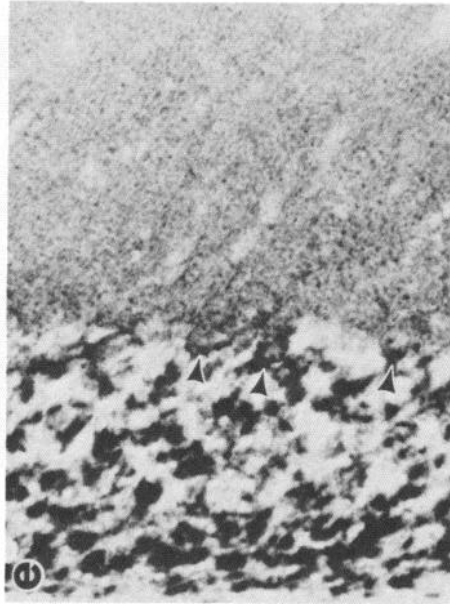
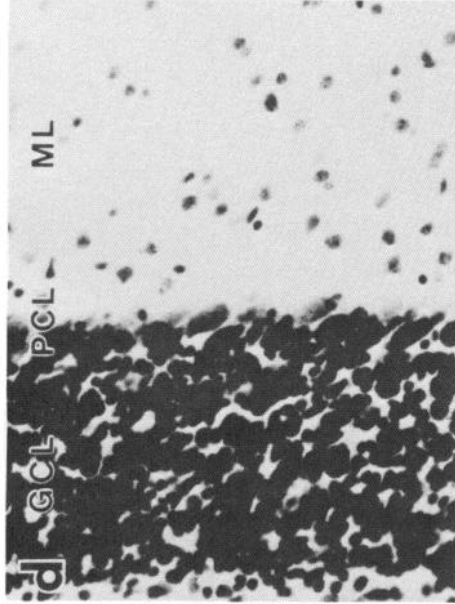
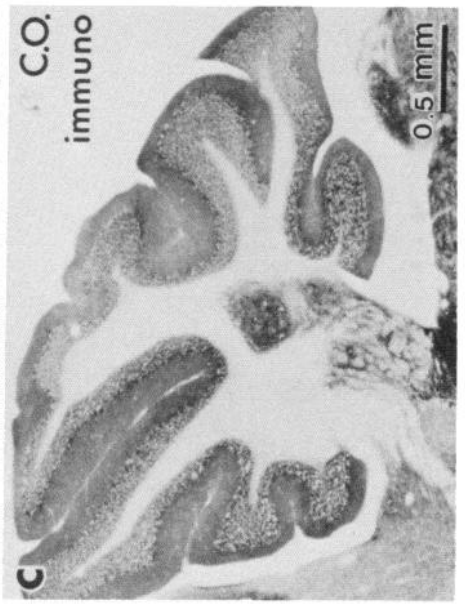


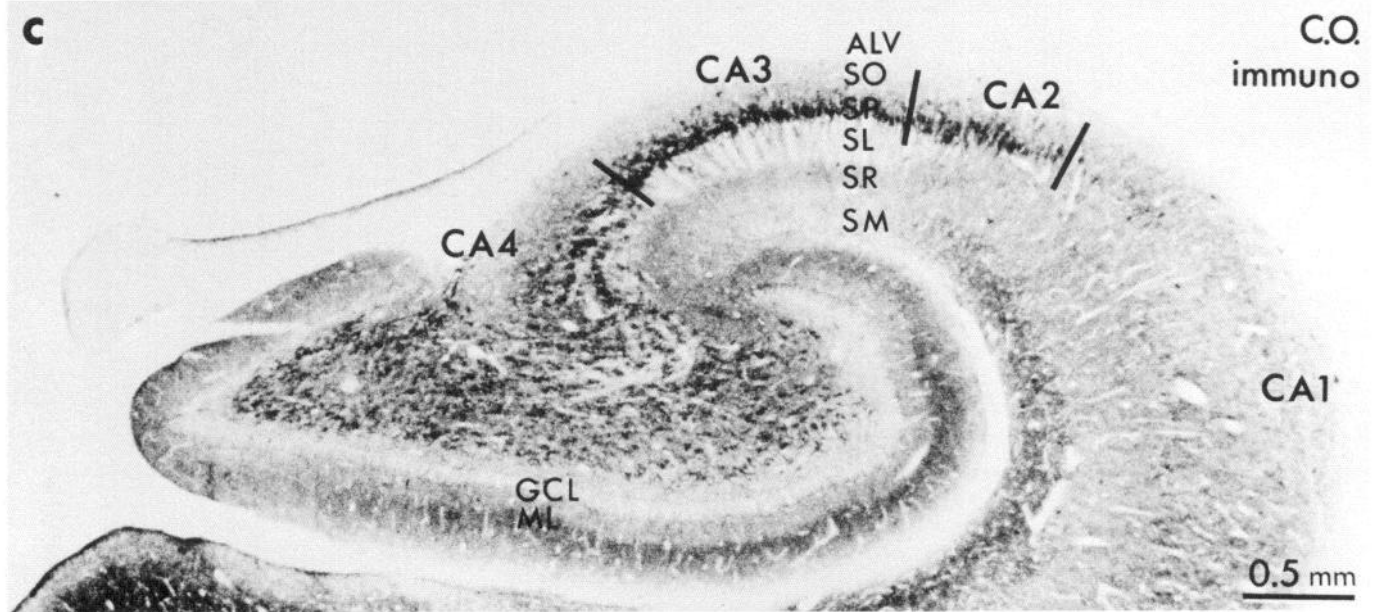
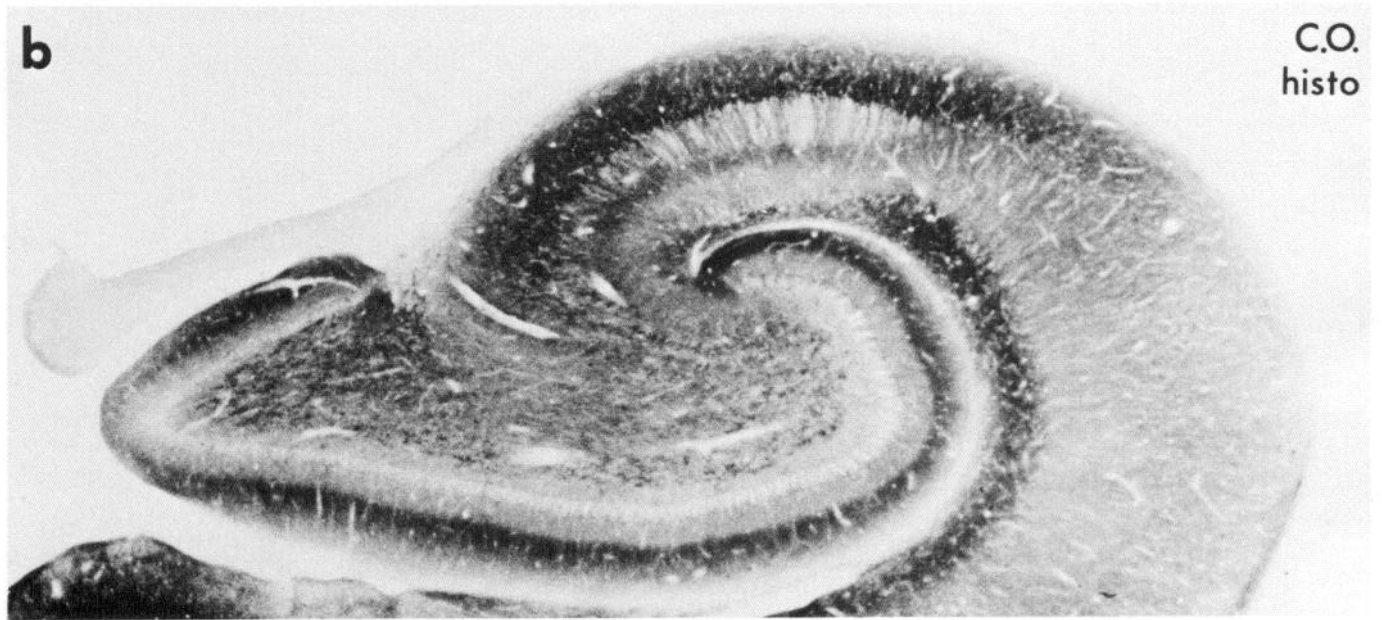
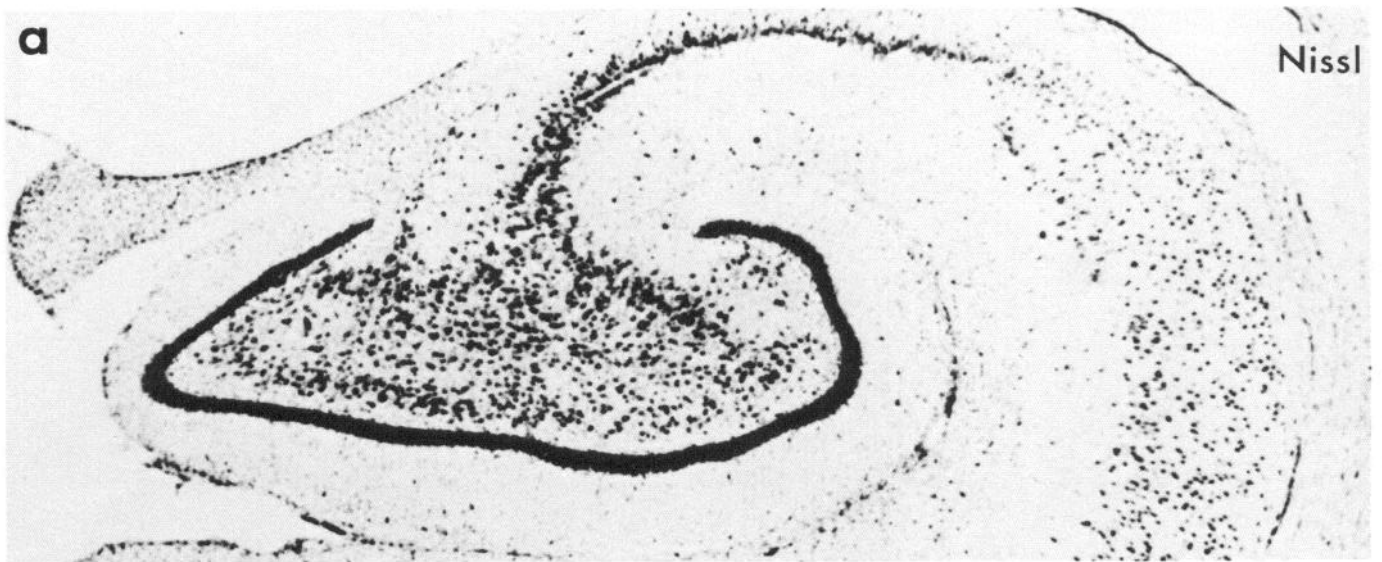
**Figure 9.** Correlation of CO activity and amount distributions in the mouse olfactory bulb. Neighboring coronal frozen sections ( $20\ \mu\text{m}$ ) processed for CO histochemistry (*a*) and CO immunohistochemistry (*b*) are shown. Section *b* was incubated with anti-CO at 1:2000 and visualized with fluorescent second and third antibodies. The arrowheads indicate adjacent glomeruli, which stained with different intensities. ONL, olfactory nerve layer; GL, glomerular layer; EPL, external plexiform layer; MBL, mitral body layer; IPL, internal plexiform layer; GRL, granule cell layer.

1982), the darkly stained part of the dentate molecular layer receives strong excitatory synaptic input from the perforant pathway (Swanson, 1982).

The patterns of CO histochemistry and immunohistochemistry in hippocampal subfield CA3 also were distinctive and followed the previously described histochemical pattern (Kageyama and Wong-Riley, 1982). Neurons of the pyramidal cell layer were darkly stained for CO activity and amount, as were

**Figure 10.** Correlation of CO activity and amount distributions in the mouse cerebellum. Adjacent parasagittal frozen sections ( $20\ \mu\text{m}$ ) were stained with cresyl violet (*a, d, g*), CO histochemistry (*b, e, h*), or CO immunohistochemistry (*c, f, i*). The section stained by CO immunohistochemistry was incubated with anti-CO at 1:8000, then processed with GaR-HRP and DAB. Views of the cerebellar cortex (*d-f*) and deep nuclei (*g-i*) are higher magnifications of the corresponding sections shown in *a-c*. The arrowheads in *e* and *f* indicate dense labeling around (but not in) the Purkinje cell bodies. The labeling probably corresponds to basket cell terminals. The arrows in *f* indicate cell bodies stained immunohistochemically (but not histochemically) in the molecular layer. ML, molecular layer; PCL, Purkinje cell layer; GCL, granule cell layer.





their apical dendrites, which ascended through the overlying stratum lucidum. The stratum lucidum was relatively unreactive except for the pyramidal cell apical dendrites. The stratum radiatum and the stratum oriens had moderate levels of CO amount and activity. These regional differences in CO activity and amount were unrelated to the density of cells in CA3, as seen by comparison with the Nissl-stained section.

To summarize the immunohistochemical results, strong correlations were observed between the distributions of CO histochemical activity and immunohistochemical amount in each brain region examined. The correlations were observed in several brain regions from two mammalian species. Other patterns within the tissues, such as the distribution of cells, differed from the pattern of CO distribution.

## Discussion

### *CO purification from brain*

CO has been isolated from porcine brain for use in analytical studies (Kuhn-Nentwig and Kadenbach, 1985; Kadenbach et al., 1986) but is more easily isolated from other organs. Purification of brain CO was considered necessary for this study because immunochemical differences exist among CO from different tissues, including brain (Kuhn-Nentwig and Kadenbach, 1985). The tissue-specific immunochemical properties of CO, along with other evidence, suggest that CO exists as several isozymes in mammals (Kadenbach et al., 1986, 1987).

The possibility that brain tissue might itself contain more than one isozyme of CO was considered. More than one isozyme of other metabolic enzymes, including lactate dehydrogenase (Maker et al., 1972) and 6-phosphofructo-1-kinase (Dunaway and Kasten, 1988), are present in brain tissue. We were able to detect only one isozyme of CO in brain by electrophoretic comparison of subunit profiles of CO from synaptic and nonsynaptic mitochondria.

The purity of our CO preparations was confirmed by heme a/protein ratio and by gel electrophoresis. Data from protein sequencing (Meinecke and Buse, 1985) and gel electrophoresis (Kadenbach et al., 1983) are consistent in indicating that 12–13 subunits are present in bovine heart CO and that the specific heme a content is 10 nmol heme a/mg protein. Disagreement does exist, however, over both the subunit composition (Kadenbach et al., 1983, 1987; Saraste, 1983) and the specific heme a content (Hartzell et al., 1978; Ozawa et al., 1982; Meinecke and Buse, 1985) of the purified enzyme. The activity of the purified enzyme was low but was restored by activation with soybean lecithin (Fig. 3), indicating that delipidation rather than denaturation was responsible for the low activity (Robinson and Capaldi, 1977).

### *Antibody specificity*

Antibodies against CO were detected by their abilities to bind CO in ELISA assays (Fig. 5a) and to immunoprecipitate active,

solubilized CO (Fig. 5b). The antibodies were highly specific in SDS immunoblots for subunit IV of the enzyme, less reactive with subunits I and II, and unreactive with other subunits (Fig. 6a). A prevalence of antibodies to subunit IV also has been reported by other groups (Nakagawa and Miranda, 1987; Nicholls et al., 1988), although Jarausch and Kadenbach (1982) succeeded in generating antibodies to all of the subunits. The antibodies reacted with CO subunit IV from several mammalian species besides cow (Fig. 6b), indicating that this protein has been conserved. The antibodies furthermore cross-react not only in blots but also immunohistochemically with cat and rat brain CO (R. F. Hevner, X. Luo, and M. T. T. Wong-Riley, unpublished observations), as well as with monkey and mouse brain CO (this study). We have not tested nonmammalian species for cross-reactivity.

Immunohistochemical specificity of the antibodies was confirmed by the absence of staining when preabsorbed anti-CO or preimmune serum was substituted for anti-CO (Fig. 7). Also, the only immunoreactive peptide detectable in SDS-solubilized brain tissue was CO subunit IV (Fig. 6, a, b). Our conclusion that the antibodies were CO-specific was reinforced by the correlation found between the histochemical and immunohistochemical distributions of CO (Figs. 8–11).

It could be argued that the immunohistochemical distribution of subunit IV might not match that of CO holoenzyme. Subunit IV, however, has a 1:1 stoichiometric ratio with purified CO holoenzyme (Merle and Kadenbach, 1980), so their distributions should match. Newly synthesized subunit IV, not yet incorporated into CO holoenzyme at the time of tissue fixation, might also be detected immunohistochemically, but since CO turns over with a half-life of 5–7 days (rat liver, *in vivo*; Ip et al., 1974), the proportion of unincorporated, newly synthesized subunit IV in tissue is probably insignificant in most areas.

The results of our biochemical and immunohistochemical studies suggest that the antibodies specifically label CO, whether active or inactive, in immunohistochemistry. Biochemically, the antibodies recognize (precipitate) active CO in solution and bind to inactive enzyme subunits in immunoblots. The immunohistochemical controls show that the labeling is specific in tissue sections. The local intensity of immunohistochemical staining thus shows the relative distribution of CO molecules.

### *Correlation of CO amount and activity*

Our immunohistochemical results (Figs. 8–11) show that regions of neural tissue rich in CO histochemical activity are also rich in CO immunohistochemical amount. This conclusion is general, since the results were similar in all regions examined in the 2 species and have been confirmed in other regions and other species (R. F. Hevner et al., unpublished observations). Our findings indicate that the local activity of CO is determined mainly by the local distribution of enzyme molecules rather than by modulation of enzyme turnover number.

←

**Figure 11.** Correlation of CO activity and amount distributions in the monkey hippocampus. Neighboring frozen sections (30  $\mu$ m) were cut perpendicular to the long axis of the hippocampus and stained with cresyl violet (*a*), CO histochemistry (*b*), or CO immunohistochemistry (*c*). The section in *c* was incubated with anti-CO at 1:4000, then processed with GaR-HRP and DAB. Note the correspondence between the histochemical and immunohistochemical labeling in stratum moleculare of CA1, stratum pyramidale of CA3, stratum radiatum of CA3, and especially in the dentate molecular and granule cell layers. The dentate molecular layer appears homogeneous in the Nissl stain but has higher levels of CO histochemical activity and immunohistochemical amount in its outer portion relative to its inner portion. *ALV*, alveus; *SO*, stratum oriens; *SP*, stratum pyramidale; *SL*, stratum lucidum; *SR*, stratum radiatum; *SM*, stratum moleculare; *ML*, molecular layer of dentate gyrus; *GCL*, granule cell layer.

The correlation between the histochemical and the immunohistochemical distributions of CO could also be explained by postulating that the antibodies recognize only active CO. However, the antibodies recognized isolated (enzymatically inactive) CO subunits in immunoblots (Fig. 6). Furthermore, the antibodies are polyclonal and probably recognize several epitopes. It is unlikely that any modifications of the enzyme affecting its turnover number would influence all or most of the epitopes.

Differences were seen between the histochemical and immunohistochemical patterns. Less contrast in staining intensity among different regions of a tissue section was present in immunohistochemistry than in histochemistry. The lower contrast can be partly attributed to the background staining always present in immunohistochemistry. Also, the signal: noise ratio of the immunohistochemistry may be less than that of the histochemistry if fewer CO molecules bind antibody than react histochemically. Another difference between the two methods was that cell bodies were sometimes more intensely labeled immunohistochemically than histochemically. For example, in the cerebellar cortex, somata in the molecular layer were stained immunohistochemically but not histochemically (Fig. 10). This cellular staining could be due to newly synthesized subunit IV, since this subunit is encoded in the nuclear genome (only subunits I–III are mitochondrially encoded) and presumably translated on ribosomes in the soma before incorporation into mitochondria and active enzyme. Another possibility is that a cell body protein cross-reacts immunohistochemically, but this seems unlikely, since not all cell bodies were stained.

Finally, it is possible that local regulation of the turnover number of the enzyme could account for each of the histochemical/immunohistochemical differences. A role for turnover number regulation cannot be excluded but would probably be minor under normal conditions, given the close match found between CO amount and activity. Indeed, the differences between the histochemical and immunohistochemical patterns may not have been significant, considering that the two methods showed nearly identical patterns in complex tissues.

#### *Distribution of energy metabolic capacity in neural tissue*

CO is not the only indicator that the capacity for generating metabolic energy varies among neural tissue regions. Other energy metabolic enzymes show activity or amount distribution patterns similar to those of CO. For example, succinate dehydrogenase (Killackey et al., 1976) and citrate synthase (Dietrich et al., 1981) have, like CO, higher activity levels in the barrel hollows of the mouse somatosensory cortex layer IV than in the septa or surrounding cortex. Also, the distribution of hexokinase (both immunohistochemical amount and histochemical activity) in the cerebellar cortex (Wilkin and Wilson, 1977) closely resembles that of CO. The results of this study confirm that not only the activity of a metabolic enzyme but also the concentration of enzyme molecules can vary locally and confer different metabolic capacities on regions of neural tissue.

Our results, furthermore, suggest that the concentration of CO molecules varies among processes and segments of processes within individual neurons. Previous studies at the electron microscopic level have found that CO activity does vary among different segments of the same neuron. For example, dentate granule cells have high CO activity levels in their distal apical dendrites in the outer molecular layer but low levels in their proximal dendrites in the inner molecular layer (Kageyama and Wong-Riley, 1982). The outer molecular layer of the dentate

gyrus is also rich in CO amount relative to the inner molecular layer (Fig. 11). This suggests that the dentate granule cell distal apical dendrites are enriched in CO molecules relative to proximal dendrites of the same neurons.

Similar arguments suggest that CO amount varies among processes and segments of individual neurons in the mouse somatosensory barrels and in the mouse cerebellum. In the barrels, CO activity is higher in dendrites in the hollows than in cell bodies in the septa (Wong-Riley and Welt, 1980). In the adult cerebellum, Purkinje cells have high CO activity in their dendrites relative to lower levels in their somata (Mjaatvedt and Wong-Riley, 1988). The pattern of CO immunohistochemistry matched that of CO histochemistry in both of these regions (Figs. 8, 10), suggesting again that the intracellular distribution of CO amount, like that of CO activity, might be nonhomogeneous. Verification of this will require CO immunocytochemistry at the electron microscopic level.

A nonhomogeneous distribution of CO molecules in individual neurons implies the existence of a mechanism for distributing CO molecules differentially among processes and their segments. The intracellular distribution of CO amount could be determined simply by the distribution of mitochondria, or mitochondria could be evenly distributed but contain different amounts of CO. Histochemically, individual mitochondria do differ in their relative CO activity, and more reactive mitochondria usually are found in tissue regions that appear more reactive at the light microscopic level (reviewed in Wong-Riley, 1989).

Whatever the mechanisms may be for distributing CO (or other energy metabolic enzymes) within cells and tissue, we think that such mechanisms probably are coupled to energy demand and thus indirectly to neural functional activity.

#### *Regulation of energy metabolic capacity*

The capacity for generating metabolic energy, as demonstrated by CO histochemistry, not only is unevenly distributed but also can change in response to alterations in neural functional activity (reviewed in Wong-Riley, 1989). We recently found in the primate visual system that not just the activity but the amount of CO is regulated by neural functional activity. Monocular retinal impulse blockage with TTX causes CO activity as well as immunoreactivity to decline in LGN laminae and cortical columns corresponding to the TTX-injected eye (R. F. Hevner and M. T. T. Wong-Riley, unpublished observations). The results of our studies indicate that the quantity and distribution of CO in neural tissue probably are determined by the level and pattern, respectively, of functional activity.

The CO immunohistochemical method should serve as a useful complement to CO histochemistry in future studies of brain energy metabolism and functional anatomy. For example, the relation between CO and other molecules can be investigated by double-label immunohistochemistry. We have used this method to investigate the relation between GABA and CO in the cat brain (Luo et al., 1989). We have also applied this method in studies, currently in progress, of cultured cells and of developing animals.

## References

- Bradford, M. M. (1976) A rapid and sensitive method for the quantitation of microgram quantities of protein utilizing the principle of protein-dye binding. *Anal. Biochem.* 72: 248–254.

- Broger, C., K. Bill, and A. Azzi (1986) Affinity chromatography purification of cytochrome-*c* oxidase from bovine heart mitochondria and other sources. *Methods Enzymol.* 126: 64–72.
- Carroll, E. W., and M. T. T. Wong-Riley (1984) Quantitative light and electron microscopic analysis of cytochrome oxidase-rich zones in the striate cortex of the squirrel monkey. *J. Comp. Neurol.* 222: 1–17.
- Cohen, P. (1980a) Well-established systems of enzyme regulation by reversible phosphorylation. In *Recently Discovered Systems of Enzyme Regulation by Reversible Phosphorylation*, P. Cohen, ed., pp. 1–10, Elsevier/North-Holland, Amsterdam.
- Cohen, P. (1980b) Protein phosphorylation and the co-ordinated control of intermediary metabolism. In *Recently Discovered Systems of Enzyme Regulation by Reversible Phosphorylation*, P. Cohen, ed., pp. 255–268, Elsevier/North-Holland, Amsterdam.
- Dietrich, W. D., D. Durham, O. H. Lowry, and T. A. Woolsey (1981) Quantitative histochemical effects of whisker damage on single identified cortical barrels in the adult mouse. *J. Neurosci.* 1: 929–935.
- Dion, A. S., and A. A. Pomenti (1983) Ammoniacal silver staining of proteins: Mechanism of glutaraldehyde enhancement. *Anal. Biochem.* 129: 490–496.
- Dunaway, G. A., and T. P. Kasten (1988) Physiological implications of the alteration of 6-phosphofructo-1-kinase isozyme pools during brain development and aging. *Brain Res.* 456: 310–316.
- Errede, B., M. D. Kamen, and Y. Hatefi (1978) Preparation and properties of complex IV (ferrocyanochrome *c*: oxygen oxidoreductase EC 1.9.3.1). *Methods Enzymol.* 53: 40–47.
- Hartzell, C. R., H. Beinert, B. F. van Gelder, and T. E. King (1978) Preparation of cytochrome oxidase from beef heart. *Methods Enzymol.* 53: 54–66.
- Hartzell, C. R., H. Beinert, G. T. Babcock, S. I. Chan, G. Palmer, and R. A. Scott (1988) Heterogeneity in an isolated membrane protein. *FEBS Lett.* 236: 1–4.
- Hatefi, Y. (1978) Preparation and properties of dihydroubiquinone: cytochrome *c* oxidoreductase (complex III). *Methods Enzymol.* 53: 35–40.
- Hendrickson, A. E., and J. R. Wilson (1979) A difference in [<sup>14</sup>C]deoxyglucose autoradiographic patterns in striate cortex between Macaca and Saimiri monkeys following monocular stimulation. *Brain Res.* 170: 353–358.
- Hevner, R. F., and M. T. T. Wong-Riley (1987) Purification of bovine brain cytochrome oxidase from synaptosomal and non-synaptosomal mitochondria. *Soc. Neurosci. Abstr.* 13: 647.
- Horton, J. C. (1984) Cytochrome oxidase patches: A new cytoarchitectonic feature of monkey visual cortex. *Phil. Trans. R. Soc. Lond. B* 304: 199–253.
- Horton, J. C., and D. H. Hubel (1981) Regular patchy distribution of cytochrome oxidase staining in primary visual cortex of macaque monkey. *Nature* 292: 762–764.
- Hurn, B. A. L., and S. M. Chantler (1980) Production of reagent antibodies. *Methods Enzymol.* 70: 104–142.
- Ip, M. M., P. Y. Chee, and R. W. Swick (1974) Turnover of hepatic mitochondrial ornithine aminotransferase and cytochrome oxidase using [<sup>14</sup>C]carbonate as tracer. *Biochim. Biophys. Acta* 354: 29–38.
- Jacobs, E. E., and D. R. Sanadi (1960) The reversible removal of cytochrome *c* from mitochondria. *J. Biol. Chem.* 235: 531–534.
- Jacobs, E. E., E. C. Andrews, W. Cunningham, and F. L. Crane (1966a) Membrane cytochrome oxidase: Purification, properties, and reaction characteristics. *Biochem. Biophys. Res. Commun.* 25: 87–95.
- Jacobs, E. E., F. H. Kirkpatrick, Jr., E. C. Andrews, W. Cunningham, and F. L. Crane (1966b) Lipid-free soluble cytochrome oxidase: Purification, properties, and reaction characteristics. *Biochem. Biophys. Res. Commun.* 25: 96–104.
- Jaraus, J., and B. Kadenbach (1982) Tissue-specificity overrides species-specificity in cytoplasmic cytochrome *c* oxidase polypeptides. *Hoppe Seylers Z. Physiol. Chem.* 363: 1133–1140.
- Johnson, D. A., J. W. Gautsch, J. R. Sportsman, and J. H. Elder (1984) Improved technique utilizing nonfat dry milk for analysis of proteins and nucleic acids transferred to nitrocellulose. *Gene Anal. Tech.* 1: 3–8.
- Johnstone, A., and R. Thorpe (1982) *Immunochemistry in Practice*, Blackwell, Oxford.
- Kadenbach, B., J. Jaraus, R. Hartmann, and P. Merle (1983) Separation of mammalian cytochrome *c* oxidase into 13 polypeptides by a sodium dodecyl sulfate-gel electrophoretic procedure. *Anal. Biochem.* 129: 517–521.
- Kadenbach, B., A. Stroh, M. Ungibauer, L. Kuhn-Nentwig, U. Buge, and J. Jaraus (1986) Isozymes of cytochrome *c* oxidase: Characterization and isolation from different tissues. *Methods Enzymol.* 126: 32–45.
- Kadenbach, B., L. Kuhn-Nentwig, and U. Buge (1987) Evolution of a regulatory enzyme: Cytochrome-*c* oxidase (complex IV). *Curr. Topics Bioenerg.* 15: 113–161.
- Kageyama, G. H., and M. T. T. Wong-Riley (1982) Histochemical localization of cytochrome oxidase in the hippocampus: Correlation with specific neuronal types and afferent pathways. *Neuroscience* 7: 2337–2361.
- Kennedy, C., M. H. Des Rosiers, O. Sakurada, M. Shinohara, M. Reivich, J. W. Jehle, and L. Sokoloff (1976) Metabolic mapping of the primary visual system of the monkey by means of the autoradiographic [<sup>14</sup>C]deoxyglucose technique. *Proc. Natl. Acad. Sci. USA* 73: 4230–4234.
- Killackey, H. P., G. Belford, R. Ryugo, and D. K. Ryugo (1976) Anomalous organization of thalamocortical projections consequent to vibrissae removal in the newborn rat and mouse. *Brain Res.* 104: 309–315.
- Krnjevic, K. (1975) Coupling of neuronal metabolism and electrical activity. In *Brain Work: The Coupling of Function, Metabolism, and Blood Flow in the Brain*, D. H. Ingvar and N. A. Lassen, eds., pp. 65–78, Academic, New York.
- Kuhn-Nentwig, L., and B. Kadenbach (1985) Isolation and properties of cytochrome *c* oxidase from rat liver and quantification of immunological differences between isozymes from various rat tissues with subunit-specific antisera. *Eur. J. Biochem.* 149: 147–158.
- Lai, J. C. K., and J. B. Clark (1979) Preparation of synaptic and nonsynaptic mitochondria from mammalian brain. *Methods Enzymol.* 55: 51–60.
- Livingstone, M. S., and D. H. Hubel (1984) Anatomy and physiology of a color system in the primate visual cortex. *J. Neurosci.* 4: 309–356.
- Luo, X. G., R. F. Hevner, and M. T. T. Wong-Riley (1989) Double labeling of cytochrome oxidase and gamma aminobutyric acid in central nervous system neurons of adult cats. *J. Neurosci. Meth.* (in press).
- Maker, H. S., G. M. Lehrer, S. Weissbarth, and M. B. Bornstein (1972) Changes in LDH isoenzymes of brain developing *in situ* and *in vitro*. *Brain Res.* 44: 189–196.
- Meinecke, L., and G. Buse (1985) Studies on cytochrome *c* oxidase, XII. Isolation and primary structure of polypeptide VIb from bovine heart. *Biol. Chem. Hoppe Seyler* 366: 687–694.
- Merle, P., and B. Kadenbach (1980) The subunit composition of mammalian cytochrome *c* oxidase. *Eur. J. Biochem.* 105: 499–507.
- Merle, P., J. Jaraus, M. Trapp, R. Scherka, and B. Kadenbach (1981) Immunological and chemical characterization of rat liver cytochrome *c* oxidase. *Biochim. Biophys. Acta* 669: 222–230.
- Mjaatvedt, A. E., and M. T. T. Wong-Riley (1988) Relationship between synaptogenesis and cytochrome oxidase activity in Purkinje cells of the developing rat cerebellum. *J. Comp. Neurol.* 277: 155–182.
- Nakagawa, M., and A. F. Miranda (1987) A monoclonal antibody against cytochrome *c* oxidase distinguishes cardiac and skeletal muscle mitochondria. *Exp. Cell Res.* 168: 44–52.
- Nicholls, P., C. E. Cooper, B. Leece, J. A. Freedman, and S. H. P. Chan (1988) Antibodies as probes of cytochrome oxidase structure and function. In *Oxidases and Related Redox Systems*, T. E. King, H. S. Mason, and M. Morrison, eds., pp. 637–651, Liss, New York.
- Ozawa, T., M. Tanaka, and T. Wakabayashi (1982) Crystallization of mitochondrial cytochrome oxidase. *Proc. Natl. Acad. Sci. USA* 79: 7175–7179.
- Read, S. M., and D. H. Northcote (1981) Minimization of variation in the response to different proteins of the Coomassie blue G dye-binding assay for protein. *Anal. Biochem.* 116: 53–64.
- Rendon, A., and A. Masmoudi (1985) Purification of non-synaptic and synaptic mitochondria and plasma membranes from rat brain by a rapid Percoll gradient procedure. *J. Neurosci. Methods* 14: 41–51.
- Robinson, N. C., and R. A. Capaldi (1977) Interaction of detergents with cytochrome *c* oxidase. *Biochemistry* 16: 375–381.
- Saraste, M. (1983) How complex is a respiratory complex? *Trends Biochem. Sci.* 8: 139–142.

- Schimke, R. T., and D. Doyle (1970) Control of enzyme levels in animal tissues. *Annu. Rev. Biochem.* 39: 929–976.
- Sokoloff, L. (1984) *Metabolic Probes of Central Nervous System Activity in Experimental Animals and Man*, Sinauer, Sunderland, Mass.
- Surovia, A., D. Pain, and M. I. Khan (1982) Protein A: Nature's universal anti-antibody. *Trends Biochem. Sci.* 7: 74–76.
- Swanson, L. W. (1982) Normal hippocampal circuitry: Anatomy. *Neurosci. Res. Prog. Bull.* 20: 624–634.
- Tootell, R. B. H., M. S. Silverman, S. L. Hamilton, R. L. De Valois, and E. Switkes (1988) Functional anatomy of macaque striate cortex. III. *Color. J. Neurosci.* 8: 1569–1593.
- Towbin, H., T. Staehelin, and J. Gordon (1979) Electrophoretic transfer of proteins from polyacrylamide gels to nitrocellulose sheets: Procedure and some applications. *Proc. Natl. Acad. Sci. USA* 76: 4350–4354.
- Vanneste, W. H. (1966) Molecular proportion of the fixed cytochrome components of the respiratory chain of Keilin-Hartree particles and beef heart mitochondria. *Biochim. Biophys. Acta* 113: 175–178.
- Vik, S. B., and R. A. Capaldi (1980) Conditions for optimal electron transfer activity of cytochrome *c* oxidase isolated from beef heart mitochondria. *Biochem. Biophys. Res. Commun.* 94: 348–354.
- Wharton, D. C., and A. Tzagoloff (1967) Cytochrome oxidase from beef heart mitochondria. *Methods Enzymol.* 10: 245–250.
- Wilkin, G. P., and J. E. Wilson (1977) Localization of hexokinase in neural tissue: Light microscopic studies with immunofluorescence and histochemical procedures. *J. Neurochem.* 29: 1039–1051.
- Wong-Riley, M. (1979) Changes in the visual system of monocularly sutured or enucleated cats demonstrable with cytochrome oxidase histochemistry. *Brain Res.* 171: 11–28.
- Wong-Riley, M. T. T. (1989) Cytochrome oxidase: An endogenous metabolic marker for neuronal activity. *Trends Neurosci.* 12: 94–101.
- Wong-Riley, M. T. T., and C. Welt (1980) Histochemical changes in cytochrome oxidase of cortical barrels after vibrissal removal in neonatal and adult mice. *Proc. Natl. Acad. Sci. USA* 77: 2333–2337.
- Woolsey, T. A., and H. van der Loos (1970) The structural organization of layer IV in the somatosensory region (SI) of mouse cerebral cortex. The description of a cortical field composed of discrete cytoarchitectonic units. *Brain Res.* 17: 205–242.
- Wray, W., T. Boulikas, V. P. Wray, and R. Hancock (1981) Silver staining of proteins in polyacrylamide gels. *Anal. Biochem.* 118: 197–203.